Contact-Limited Hole Current in Poly(p-phenylenevinylene)

Blom, P.W.M.; Vissenberg, M.C.J.M.; Black, D.W.

Published in:
EPRINTS-BOOK-TITLE

Publication date:
2002

15
Contact-Limited Hole Current in Poly(*p*-phenylenevinylene)

P. W. M. Blom
University of Groningen, Groningen, The Netherlands

D. W. Black
Philips Research Laboratories, Eindhoven, The Netherlands, and University of Glasgow, Glasgow, United Kingdom

M. C. J. M. Vissenberg
Philips Research Laboratories, Eindhoven, The Netherlands

I. INTRODUCTION

Due to their application in electroluminescent devices, conjugated polymers have been the subject of intense research over the decade. A typical polymer light-emitting diode (PLED) consists of a thin layer of undoped conjugated polymer, such as poly(phenylenevinylene) (PPV), sandwiched between two electrodes on top of a glass substrate. As the anode a patterned indium-tin-oxide (ITO) bottom electrode is used, whereas the cathode on top of the polymer consists of an evaporated Ca electrode, as indicated in Figure 1. Under forward bias electrons and holes are injected into the polymer from the cathode and anode, respectively.

During the injection process, charge carriers have to surmount or tunnel through a contact barrier that arises from the band offset between the polymer and the electrodes. For the ITO anode, which matches relatively well with the highest occupied molecular orbitals of PPV, a low contact barrier for hole injection of around 0.2 eV is expected [1]. For efficient electron injection, on the other hand, low work function metals such as Ca,

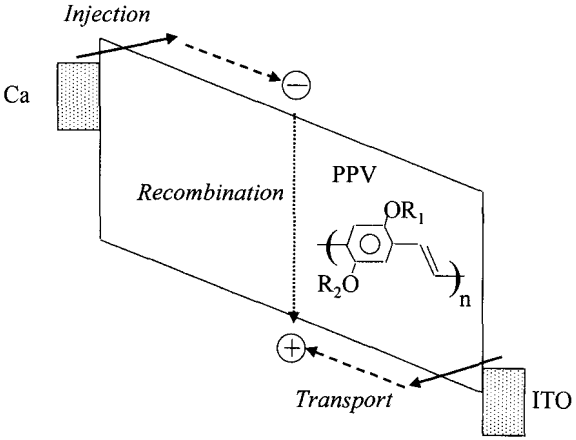

Figure 1 Schematic band diagram of a polymer light-emitting diode (PLED) under forward bias. Indicated are the three basic processes that govern the performance of the PLED: injection, transport, and recombination. The conjugated polymer used in this study is poly(dialkoxy *p*-phenylenevinylene), whereas ITO and Ca serve as the anode and cathode, respectively.

which match up with lowest unoccupied molecular orbitals of PPV, must be used. It is evident that control of the electrode-polymer interfaces is very important with regard to the device performance of a PLED. The nature of metal-polymer interfaces and their formation have been studied both experimentally and theoretically [2]. The understanding of the metal-polymer interface is complicated by the occurrence of chemical interactions, which depend on both the metal and the polymer involved; the cleanliness of the materials; and the vacuum system used in the evaporation process [2]. However, in spite of these chemical interactions, measurements of the built-in electrical field have demonstrated that the energy barriers at the electrode-polymer interfaces still scale with the work functions of the electrodes [3]. Thus, the contact barrier for a given electrode-polymer combination is still a relevant parameter for estimating the role of charge injection.

It is crucial for the understanding and optimization of polymer LEDs to obtain an answer to the question of whether the device characteristics of polymer LEDs are controlled by injection or transport. Experimentally, the discrimination between charge injection and charge transport on the basis of the device characteristics of a PLED has proven to be difficult. Initially, from the absence of a thermally activated behavior as well as a highly nonlinear *J-V* characteristic at high electric fields, it has been suggested [4,5] that the dependence of J on V resembles that of Fowler-Nordheim (F-N)

tunneling through a barrier. From the slope of the *J-V* characteristics in an F-N plot [$\ln(J/E^2)$ vs. E^{-1})], energy barriers of 0.1 and 0.2 eV were deduced for the Ca/PPV and ITO/PPV interfaces, respectively [5]. However, quantitatively the currents predicted by the F-N theory for these low-energy barriers exceed the experimentally observed currents by several orders of magnitude. Furthermore, it has been demonstrated [6] that the hole currents in our PPV-based PLEDs are determined by the bulk transport properties of the PPV and not by charge injection.

II. MODEL CALCULATION

As a first estimate of whether the current for a given polymer-electrode combination will be injection or transport limited, the effect of an injection barrier j_b on the *J-V* characteristics of a PLED has been modeled [6]. However, a major problem for setting up such a model calculation is the fact that the knowledge of the mechanisms of charge injection into conjugated polymers is not nearly as comprehensive as for inorganic semiconductors [7]. Therefore, let us first review the conventional charge injection mechanisms and then discuss their application in case of a conjugated polymer. First, we apply a bias V across a device with thickness L, which results in a current density J. As a result of the injection of charges at $x = 0$, the dependence of the electric field on the position x (between 0 and L) is given by [8]:

$$E(x) = \sqrt{E(0)^2 + \frac{2Jx}{\varepsilon_0 \varepsilon_r \mu}} \tag{1}$$

with $E(0)$ is the electric field at the contact, m the charge carrier mobility, and $e_0 e_r$ the permittivity of the semiconductor. The second term in the right-hand side of Eq. (1) takes into account the effect of space charge in the device. For a device that is strongly contact limited, only a small number of charge carriers are injected, which results in a low current. As a result, $E(0) >> 2JL/e_0 e_r m$ and the electric field $E(x) = E(0) = V/L$ is constant over the device. For efficient charge injection $E(0) \leq JL/e_0 e_r m$ and space-charge effects have to be taken into account.

A. Ohmic Contact

For an Ohmic contact, $E(0) = 0$ and the *J-V* behavior is directly given by [9]:

$$J = \frac{9}{8} e_0 e_r m \frac{V^2}{L^3} \tag{2}$$

This quadratic dependence of J on V is characteristic for the so-called space-charge limited current (SCLC). In Figure 2 the calculated bulk SCLC is shown (dashed line) for a device with L = 100 nm and m = 10^{-10} m^2/Vs, which is typical for PPV.

B. Contact Limited Current

The current density-voltage (J-V) characteristics for thermionic emission of charge from a metallic electrode into an insulator are described by the Richardson-Schottky equation [10]:

$$J = A^* T^2 \exp\left(\frac{-q f_b}{kT}\right) \tag{3}$$

where A^* is the Richardson constant ($4pqm^*k^2/h^3$), T the temperature, and j_b the barrier height arising from the band offset between the insulator and the electrode. The barrier height j_b is lowered by the image force effect:

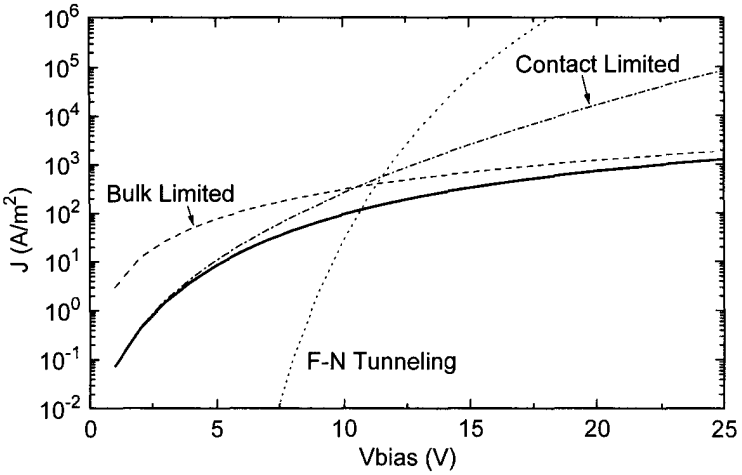

Figure 2 Calculated J-V characteristics (*solid line*) for a device with thickness L = 100 nm, an injection barrier height j_{b0} = 0.35 V, a mobility m = 10^{-10} m^2/Vs, and a dielectric constant e_r = 3. For comparison, the bulk-limited SCLC [*dashed line*, Eq. (5)], the diffusion-limited injection [*dash-dotted line*, Eqs. (2) and (3)], and the Fowler-Nordheim current [*dotted line*], assuming $F(x) = F(0) = V/L$ are included as well.

$$\phi_b = \phi_{b0} - \Delta\phi = \phi_{b0} - \sqrt{\frac{qE(0)}{4\pi\varepsilon_0\varepsilon_r}} \tag{4}$$

where $E(0)$ is the electric field at the contact. It has been pointed out by Simmons that this expression is invalid in case of an insulator with a low carrier mobility [11]. For this special case, a large amount of charge will build up at the contact such that back-diffusion from the insulator to the metal will occur. In this diffusion limited regime the *J-V* characteristics are given by [11]:

$$J = qp(0)\mu E(0) = qN_c \exp\left(\frac{-q\phi_b}{kT}\right)\mu E(0) \tag{5}$$

where $p(0)$ is the charge carrier density at the contact, μ the charge carrier mobility, and N_c the effective density of states. For a given current J, Eqs. (4) and (5) directly provide the boundary condition for the electric field $E(0)$ at the injecting contact. By integration over x using Eq. (1), the *J-V* characteristic can be obtained for arbitrary ϕ_{b0}. However, the main result of Eq. (5) is that in case of a low-mobility material it is very difficult to disentangle contact-limited and bulk-limited processes. The charge-carrier density $p(0)$ depends on the injection process, whereas the mobility, which determines the velocity of the charge carriers away from the contact, is a bulk property of the semiconductor. Therefore, for conjugated polymers, which exhibit extremely low mobilities as compared to conventional semiconductors [6], it is expected that besides the injection process the mobility still plays an important role in contact-limited devices.

In order to investigate the role of an injection barrier ϕ_{b0} in a low mobility material we have calculated the *J-V* characteristics using Eqs. (1), (4), and (5) for a device with L = 100 nm, $\mu = 10^{-10}$ m^2/Vs, ϕ_{b0} = 0.35 V, and ε_r = 3, as shown in Figure 2 (solid line). For comparison, the limiting cases for an Ohmic contact [$E(0) = 0$], implying SCLC according to Eq. (2), and diffusion-limited injection, Eqs. (4) and (5) with $E(x) = E(0) = V/L$, are also given. At low bias (V < 5 V) the calculated current is approximately equal to the diffusion-limited injection current, and at high bias (V > 15 V) the current approaches the bulk SCLC current. This transition from contact-limited current to bulk-limited current at high fields results from barrier lowering [Eq. (4)], which then eliminates the role of the injection barrier. Also plotted in Figure 2 is the result for F-N tunneling with $E(0) = V/L$. It is clear that at low bias this injection mechanism is negligible with regard to diffusion-limited injection, whereas at high bias space-charge effects dominate the conduction. In general, it will depend on both ϕ_{b0} and L whether the conduction is injection or space-charge limited. By repeating

these calculations for various injection barriers j_{b0}, it appears that for $j_{b0} \leq 0.2$ V the *J-V* characteristics are given by Eq. (2) in the whole bias regime. Thus, from this simple estimate we have obtained that an electrode with an injection barrier of ≤0.2 V at the electrode-PPV interface is able to supply the bulk SCLC. Similar conclusions have been drawn from model calculations by Malliaras and Scott [12] and Campbell et al. [13] who reported that bulk-dominated behavior in PLEDs is expected for contact barriers lower than 0.3 eV or 0.4 eV, respectively.

From the first simple estimates described above it became clear that the low charge carrier mobility of the PPV-based materials enhances the occurrence of space-charge effects in a PLED. Consequently, knowledge about the mobility is indispensable in disentangling the contributions from the bulk (mobility) and the electrode (carrier density) to the contact-limited currents in low-mobility materials. Thus, a systematic experimental study of contact-limited currents in conjugated polymers requires the use of both Ohmic contacts (for determination of the mobility) and blocking contacts (for evaluation of the injection mechanism).

It should be noted that the equations used in the calculations for charge injection so far have been derived for inorganic semiconductors with sharply defined band edges. For organic semiconductors with an energy distribution of localized states the injection mechanism is expected to be more complicated [14,15]. Alternatively, a model of thermally assisted tunneling of carriers from the contact to localized states of the polymer has been formulated [16]. This model has been further investigated by including energetic disorder and image force effects in a Monte Carlo simulation [14,17]. These simulations indicate that in conjugated polymers an increase of *J* with *V* is mainly due to the field dependence of the mobility as well as an additional increase of the carrier density at the contact due to image force effects [17]. In a recent study by Arkhipov et al. [18], charge injection from metallic electrodes into a random hopping system has been described. The mechanism consists of injection from the Fermi level of the electrode into the tail states of the distribution of hopping states of the disordered conductor, followed by either a diffusive escape from the attractive image potential or return to the electrode.

In the present study we use the conventional injection model [Eqs. (4) and (5)] to analyze the experimental injection-limited currents in PPV. In this approach the presence of localized states in the PPV is taken into account by the use of an empirical charge carrier mobility, which represents the charge transport in a disordered hopping system. From the experiments we then determine the field and temperature dependence of the metal-polymer interface charge carrier density $p(0)$. The evaluation of $p(0)$ for various

electrodes, fields, and temperatures then provides direct information about the charge injection mechanism in PPV, which is the subject of this study.

III. EXPERIMENTAL

The *J-V* characteristics of holes in PPV are investigated in both the bulk and contact-limited regime using various hole-injecting electrodes. The devices under investigation consist of a single polymer layer sandwiched between two electrodes on top of a glass substrate. The polymer is a soluble poly(dialkoxy *p*-phenylenevinylene) [6] that is spin coated on top of a patterned ITO electrode. As a top electrode we use evaporated Au, Ag, Al, and Cu contacts. From cyclovoltametric experiments it has been shown that the hole transport states of our PPV are located approximately 5.3 eV below the vacuum level (0 eV). From electroabsorption measurements on poly[2-methoxy,5-(2´-ethylhexyloxy)-1,4-phenylenevinylene) (MEH-PPV), which is very similar to our PPV, an energy of -5.35 eV has been obtained [19]. The work function of our ITO amounts to 4.8 eV, from which a contact barrier for hole injection of about 0.5 eV is expected. Figure 3 schematically shows a band diagram indicating the work functions of the various electrodes

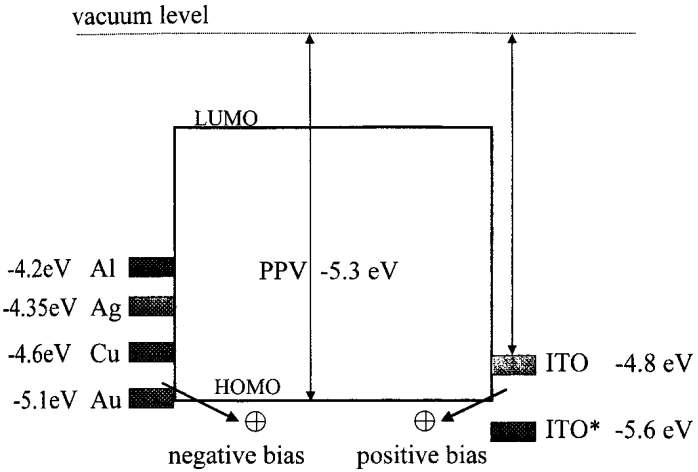

Figure 3 Band diagram indicating the work functions of the electrodes used in this study. Under forward (+) bias, holes are injected from the ITO and ITO* electrode; for negative bias (-), holes are injected from the evaporated Al, Ag, Cu, and Au electrodes, respectively. As a result of the large energy barriers with regard to the conduction band, electron injected can be neglected.

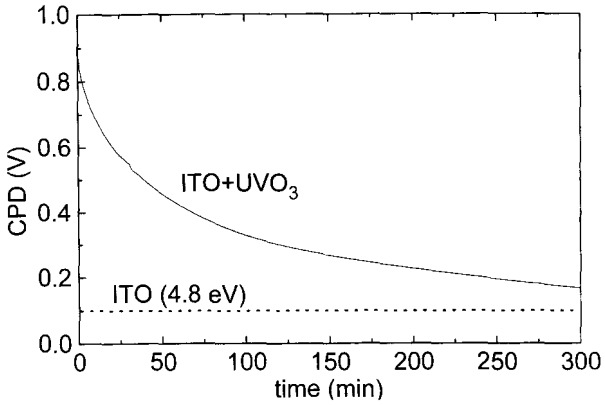

Figure 4 Contact potential difference (CPD) between the ITO and an Au reference electrode vs. time without (*dashed line*) and after UV/ozone cleaning of the ITO (*solid line*).

used in this study with regard to the transport states of PPV. By using a UV/O_3 or an O_2 plasma cleaning treatment the work function of ITO can be increased [20,21] by up to 0.8-0.9 eV, as shown in Figure 4. These measurements have been performed using a Kelvin probe in a clean-room environment. The oxidation of the ITO surface is responsible for the observed work function increase [20] and such a well-cleaned ITO contact is hereafter denoted as ITO*. An additional difficulty when studying hole injection from evaporated metallic contacts into conjugated polymers is that some metals, such as Ca and Al, chemically interact with the polymer [22-24], which may complicate the charge injection process. However, noble metals deposited on organic conductors form abrupt unreacted interfaces [25]. The *J-V* measurements are performed in a nitrogen atmosphere in the temperature range 200-300 K. For a positive bias the holes are injected from the bottom ITO or ITO* electrode, whereas a negative bias implies hole injection from the evaporated metal electrode. Furthermore, in the measured voltage range there is no light emission from the devices, indicating that the devices can be regarded as hole-only devices.

A. Ohmic Contact

For a well-cleaned ITO* contact it has been demonstrated that the *J-V* characteristics are (bulk) limited by space-charge effects [6]. This observation demonstrates that for an ITO* contact on PPV the hole current is completely governed by the bulk conduction and not by charge injection. In

Figure 5 the *J-V* characteristics for holes injected from the ITO* contact into the PPV are shown at various temperatures. The occurrence of SCLC in our ITO*/PPV devices enables us to directly obtain the *E* and *T* dependence of the hole mobility in PPV [26], given by:

$$m_p(E, T) = m_0(T)\exp(g\sqrt{E}) \tag{6}$$

with

$$m_0(T) = m_0 \exp\left(-\frac{\Delta}{k_B T}\right) \tag{7}$$

and

$$g = B\left(\frac{1}{k_0 T} - \frac{1}{k_0 T_0}\right) \tag{8}$$

with $\Delta = 0.50$ eV, $B = 3.1 \times 10^{-5}$ eV $(\mathrm{V/m})^{-1/2}$, $T_0 = 420$ K, and $m_0 = 1.0 \times 10^{-2}$ $\mathrm{m^2/Vs}$. The corresponding calculated SCL *J-V* characteristics are also shown in Figure 5. This functional form of the field *E* and temperature *T* dependence of the carrier mobility [Eq. (6)] is an intriguing feature of disordered organic semiconductors. The stretched exponential form has first been observed for poly(*N*-vinylcarbazole) by Gill in 1972 [27]. Numerous

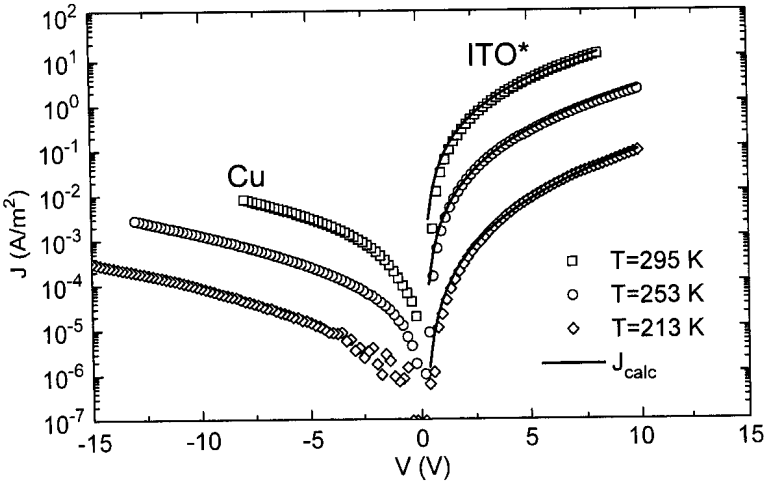

Figure 5 Forward hole current density *J* vs. voltage *V* of an Ohmic ITO* contact using a ITO*/PPV/Cu hole-only device with thickness $L = 300$ nm at various temperatures. The calculated *J-V* characteristics for positive bias following the SCLC model, using the field-dependent mobility [Eqs. (6)-(8)] are plotted as solid lines.

experimental studies on molecularly doped polymers, pendant group polymers, and amorphous molecular glasses have revealed a similar behavior [28-30].

A quantitative microscopic interpretation of this ubiquitous mobility requires a model for the charge transport in these materials. Charge transport in disordered organic conductors is thought to proceed by means of hopping in a Gaussian site-energy distribution. This density of states (DOS) reflects the energetic spread in the charge transporting levels of chain segments due to fluctuation in conjugation lengths and structural disorder. Bässler and coworkers [31,32] have performed numerical simulations of charge transport in a regular array of hopping sites with a Gaussian distribution of site energies. In this Gaussian disorder model (GDM), the following functional dependence of m has been proposed [31]:

$$m_{GDM} = m_\infty \exp\left[-\left(\frac{2s}{3k_BT}\right)^2 + C\left(\left(\frac{s}{k_BT}\right)^2 - 2.25\right)\sqrt{E}\right] \qquad (9)$$

with m_∞ the mobility in the limit $T \rightarrow \infty$, s the width of the Gaussian DOS, and C a constant (depending on, say, the site spacing). Thus, the phenomenological parameters Δ and g [Eq. (6)] may be related to the microscopic material parameter s. Applying Eq. (9) to the zero-field mobility of our PPV, as shown in Figure 6, yields for the width of the Gaussian DOS a

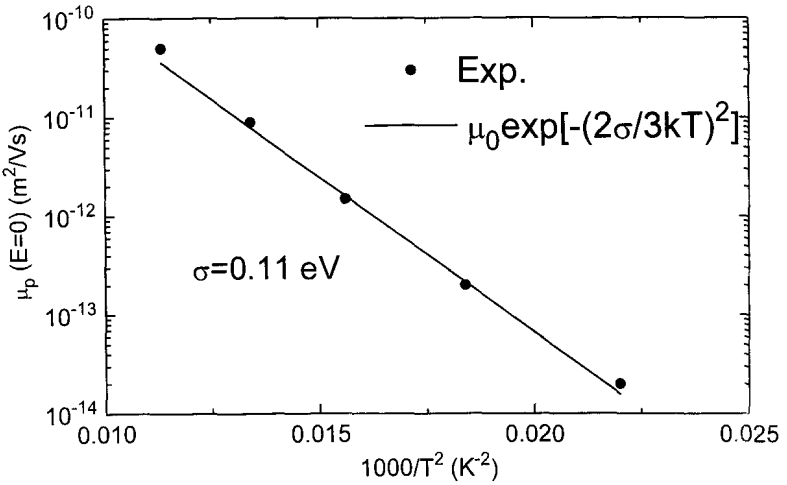

Figure 6 Zero-field mobility $m_0(T)$ vs. $1/T^2$ (symbols) as obtained from the *J-V* characteristics of the ITO* contact. From a comparison with the Gaussian disorder model [Eq. (9)], a width of the DOS of 0.1 eV is obtained (*solid line*).

value of s = 0.11 eV. The GDM simulations reproduced the $m \propto \exp(\sqrt{E})$ law only at relatively high fields (10^8 V/m). At low fields, agreement with experiments could be improved by taking into account spatial correlations between the energies of neighboring sites [33]. In an analytical one-dimensional model the form of the empirical mobility, as defined by Eqs. (6)-(8), has been attributed to energy correlations associated with charge-dipole interactions [34], which has been confirmed by simulations for three dimensions [35]. The modification of Eq. (9) by incorporation of correlation effects only slightly (<10%) affects the value of s as obtained from the zero-field mobilities in Figure 6. In a recent model using an inhomogeneity in structure instead of energy correlations [36], the stretched exponential behavior of the mobility has been reproduced in a broad field and temperature range. Here the characteristic field dependence in conjunction with the Gaussian DOS directly follows from the topology of the inhomogeneous structure. The question of which mechanisms are responsible for the ubiquitously observed mobility is a subject of ongoing research.

B. Contact-Limited Hole Currents

In the previous section it has been demonstrated that in the bulk-limited regime the hole conduction in PPV is consistently described by a combination of space-charge effects and a field-dependent mobility. In Figure 7

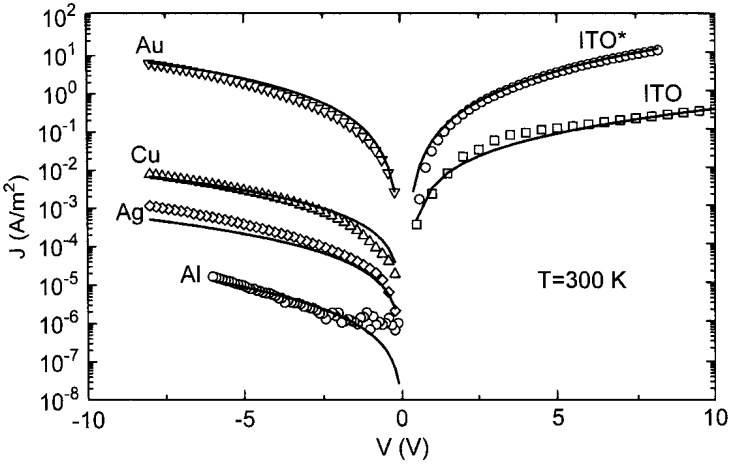

Figure 7 Experimental (*symbols*) and calculated (*solid lines*) *J-V* characteristics at T = 295 K of ITO$^{(*)}$/PPV/M hole-only devices with thickness L = 300 nm using M = Al, Ag, Cu, and Au as top electrodes.

the *J-V* characteristics of various devices are shown at T = 295 K with a thickness of the PPV film L = 300 nm. In forward bias a large difference is observed between the bulk SCLC of the cleaned ITO* and the current of the uncleaned ITO, which is therefore contact limited. In reverse also a reduction with regard to the SCLC is observed for hole injection from the evaporated metal electrodes. The amount of reduction is larger for lower work function electrodes, as expected from the energy level diagram shown in Figure 3.

In order to further investigate the injection mechanism we compare the E and T dependence of the contact-limited currents with the bulk SCLC, as shown in Figure 8 for an ITO*/PPV/Cu device. With the hole mobility $m_P(E, T)$ known, the hole density $p(0)$ at the polymer-electrode interface can be directly determined from the contact-limited currents (Au, Al, Ag, Cu, and ITO) using Eq. (5) with $E(0) = V/L$, where we have neglected the influence of space charge. In Figure 9 the E and T dependence of $p(0)$ is shown for the various electrodes. Remarkably, $p(0)$ is independent of E and T for Al, Ag, Cu, and ITO electrodes. Thus, the contact-limited *J-V* characteristics are simply described by an Ohmic-like current [Eq. (5) with $E(0)$

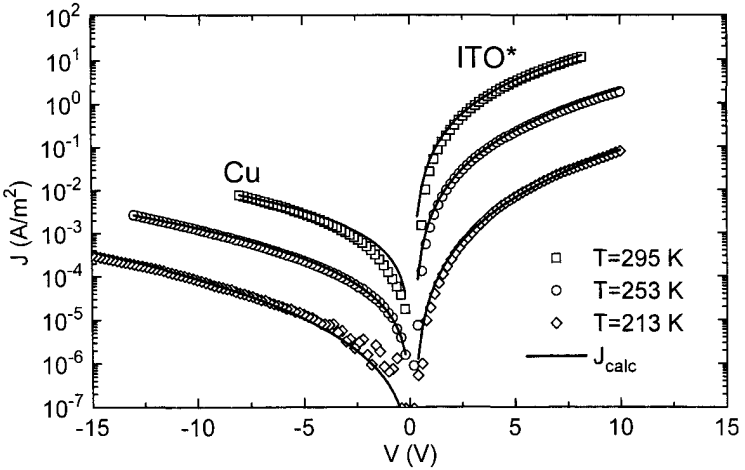

Figure 8 Current density J vs. voltage V of an ITO*/PPV/Cu hole-only device with thickness L = 300 nm for various temperatures. The calculated *J-V* characteristics for positive bias following the SCLC model using the field-dependent mobility [Eqs. (6)-(8)] are plotted as solid lines. For negative bias, the Ohmic-like *J-V* characteristics are plotted (*solid lines*) using a field- and temperature-independent hole density $p(0) = 6 \times 10^{18}$ m^{-3}.

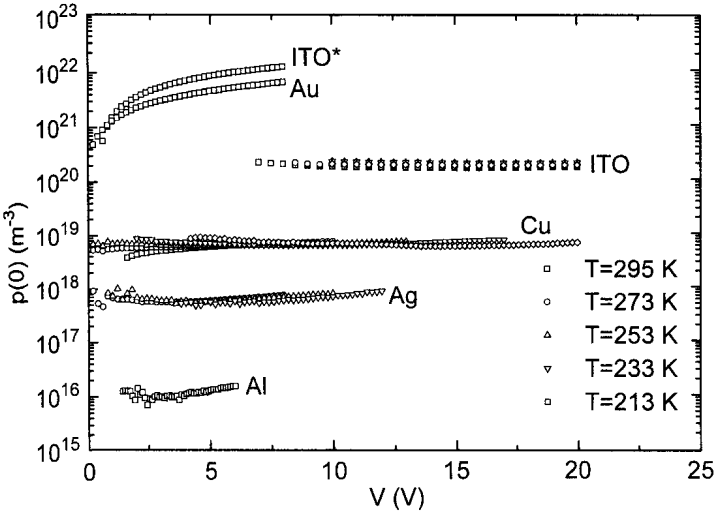

Figure 9 Hole density at the interface $p(0)$ as a function of the applied voltage for various temperatures as determined from the contact-limited currents using Eqs. (1) and (2) with $E(0) = V/L$ for the various electrodes. The hole density $p(0)$ amounts to 1.5×10^{16} m^{-3} for Al, 4.0×10^{17} m^{-3} for Ag, 6×10^{18} m^{-3} for Cu, and 2.0×10^{20} m^{-3} for uncleaned ITO. For ITO* and Au, $p(0)$ exhibits a linear voltage dependence due to space-charge effects.

$= V/L$] with a field-dependent mobility [Eqs. (6)-(8)] and a constant hole density. This is exemplified for the Cu electrode in Figure 8 by the solid lines for negative bias using a hole density $p(0) = 6 \times 10^{18}$ m^{-3}. Applying Eq. (5) to the bulk SCLC for ITO*, a linear dependence of $p(0)$ on V is observed, as expected for an SCLC where the approximation $E(x) = V/L$ no longer holds. The similar bias dependence for the Au electrode indicates that here space-charge effects are equally important. Space-charge effects can be taken into account by combining Eqs. (5) and (6) with the Poisson equation [26]. Then for the Au electrode, $p(0) = 1 \times 10^{22}$ m^{-3} is obtained, independent of E and T. In case of the ITO* electrode, the calculated J-V characteristics are, as expected for bulk-limited conduction, independent of the charge carrier density at the interface as long as $p(0) > 4 \times 10^{23}$ m^{-3}. The experimentally obtained values for $p(0)$ are plotted in Figure 10 against the work function f_M for the various electrodes. It appears that $p(0)$ varies exponentially with j_M. The observed dependence of $p(0)$ on f_M and its independence of E and T are the main results of our study.

It should be noted that an exponential behavior of $p(0)$ with j_M is also expected for the conventional thermionic injection model, in which $p(0) =$

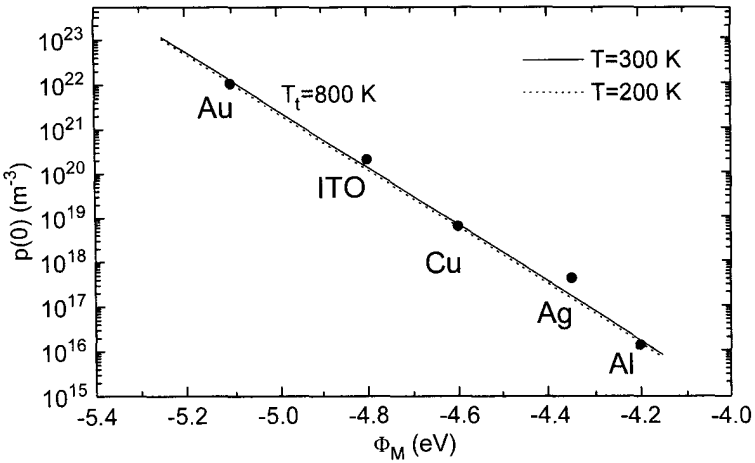

Figure 10 Experimental interface hole density $p(0)$ (*dots*) as a function of the electrode work function. By assuming an exponential distribution of localized states with a typical width kT_t (T_t = 800 K), Eqs. (10) and (11) give a direct relation between $p(0)$ and j_M (*solid line*, T = 300 K; dashed line, T = 200 K), which provides the boundary condition for hole conduction in PPV for an arbitrary electrode.

$N_v \exp(-e(j_M - j_{PPV})/kT)$ with N_v the effective density of states in the valence band. However, the observation of an E- and T-independent $p(0)$ is in strong contrast to the thermionic emission model wherein a thermally activated behavior due to the energy barrier and an additional field dependence as a result of the image force effect is expected.

IV. DISCUSSION

In order to interpret our results various additional aspects should be taken into account: First, the charge transport in a disordered organic semiconductor is governed by hopping in a distribution of localized states (DOS), rather than extended state transport [16-18,31]. Furthermore, the values obtained for $p(0)$ at the various contacts represent the magnitude of the hole density at the electrode-polymer interface but do not provide information about the charge carrier density inside the device. Let us start with the energy level diagram for a disordered semiconductor sandwiched between two identical electrodes, as shown in Figure 11. After alignment of the Fermi level the tail of the Gaussian distribution is filled with charge carriers up to the work function of the electrode. For an undoped semiconductor with a large

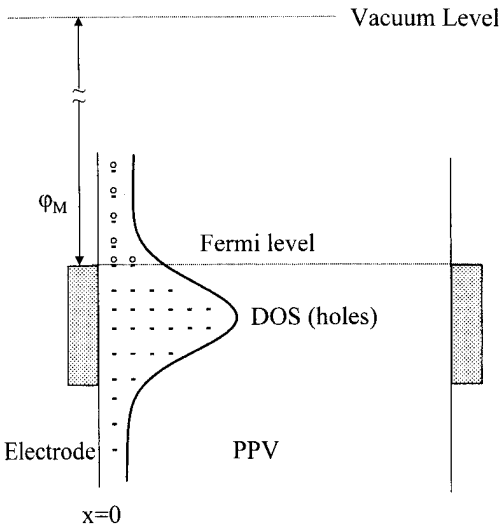

Figure 11 Schematic energy diagram for a disordered semiconductor with a distribution of localized states (DOS), sandwiched between two identical electrodes. The open circles represent the localized states occupied by a hole in order to line up the Fermi level at the interface.

band gap, which is the case for PPV, this gives rise to an accumulation region of injected charge at the contact [37]. For very thin films, as in the present study, the accumulation regions of the opposing contacts overlap, and all the charge in the bulk is of extrinsic nature. When the amount of transferred charge required for this alignment is small, band bending effects can be neglected. After application of a bias these extrinsic charge carriers provide an Ohmic-like current. As stated above, the mobility represented by Eqs. (6)-(8) reflects the hopping conduction in such a Gaussian distribution of localized states [31]. For our PPV, the width of the distribution of localized states amounts to 0.11 eV. In such a situation, the number of extrinsic charge carriers in the device would be determined by the work function of the electrodes.

Let us compare the distribution of localized states in the bulk of the PPV with the observed dependence of the interface charge $p(0)$ against j_M. The observed dependence of $p(0)$ against j_M suggests that the tail of the density of localized states at the interface $N(x)$ can be approximated by an exponential,

$$N(x) = \frac{N_t}{kT_t} \exp\left(-\frac{x}{KT_t} \right) \tag{10}$$

where x is the energy distance with regard to j_{PPV}, N_t the density of tail states, and kT_t an energy characterizing the width of the tail. The carrier density $p(0)$ at the electrode-PPV interface is now calculated using the Fermi-Dirac distribution:

$$p(0) = \int \frac{N(\xi)}{1 + \exp\left(\frac{-\xi + \phi_M - \phi_{PPV}}{kT} \right)} d\xi \tag{11}$$

In Eq. (11) we have assumed that the position of the Fermi level at the interface is solely determined by the work function of the metal j_M. Agreement with experiment is obtained for T_t = 800 K and $N_t = 4 \times 10^{23}$ m^{-3}, as shown in Figure 10 (solid line). For this characteristic distribution, the change in $p(0)$ when going from 300 to 200 K only amounts to about 15%, as shown in Figure 10 by the dashed line, which is within our experimental resolution. In Figure 12 the intrinsic Gaussian distribution of localized states

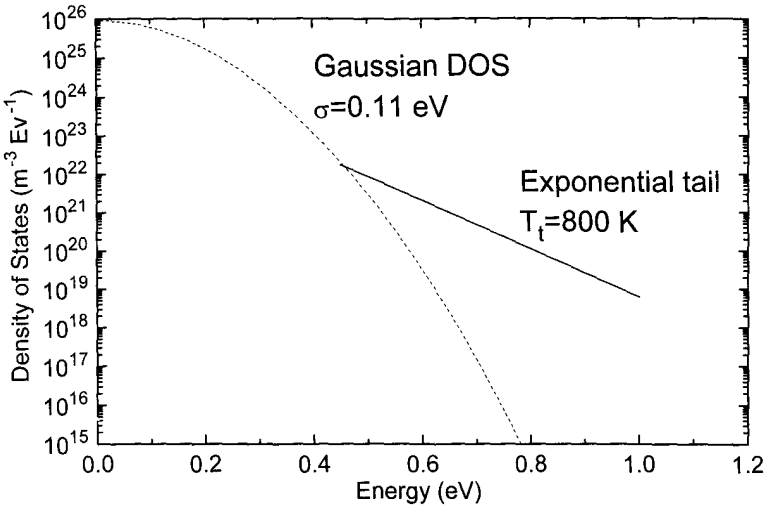

Figure 12 Density of localized states at the interface (solid line) compared to the intrinsic Gaussian DOS (dashed line) arising from energetic disorder in the PPV. For the Gaussian DOS $G(x)$, defined as $N_{site}/(\sqrt{(2p)}s)\cdot\exp(-0.5(x/s)^2)$ where x = 0 corresponds to the energy levels of the transport states of the PPV, a total site density N_{site} of 2.5×10^{25} m^{-3} has been used [6]. It appears that the interface states act as a broadened tail of the intrinisic Gaussian DOS.

is shown together with the DOS at the interface. At low temperature the interface DOS can be approximated by $p(0)/kT_t$. It appears that the experimentally observed distribution of interface states acts as a broad exponential tail which clearly differs from the intrinsic Gaussian distribution of localized states due to energetic disorder in the PPV [31]. Since we only probe the DOS at the metal-polymer interface, this additional tail may be attributed to interactions between the polymer and the metal electrode.

With regard to the charge injection mechanism in our electrode-PPV system, the experimental results strongly indicate that the exponential tail of localized states at the electrode-PPV interface acts as a charge carrier reservoir from which holes are injected into the PPV, analogous to an Ohmic contact where the charge carriers in the metal act as the reservoir, as schematically indicated in Figure 13. As a result, the strongly contact-limited hole currents in PPV show Ohmic-like *J-V* characteristics, in which the hole density is determined by the electrode work function and the density of localized states at the electrode-PPV interface. Furthermore, since the energy distribution of these localized states is large compared to *kT*, the carrier density in the reservoir only shows a weak *T* dependence. The complete set of our experimental *J-V* characteristics can now be modeled using Eqs. (5)-(8) and the Poisson equation, which describe the bulk transport, together with Eqs. (10) and (11), which provide the boundary condition relating $p(0)$ to j_M. The calculated results for the various electrodes are

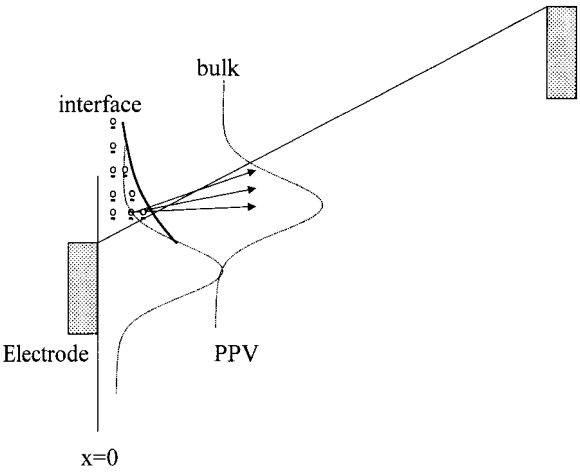

Figure 13 Schematic representation of the hole injection mechanism for the contact-limited hole devices of our study: holes are injected from the interface states, which act as a reservoir for charge injection, into the transport states of PPV.

shown in Figure 7 (solid lines), where we have used the metal work functions shown in Figure 3 as input parameters. It is demonstrated that this model provides an excellent description of the experimental *J-V* characteristics of holes in PPV as a function of voltage, temperature, and electrode work function. Thus, our model for transport of holes in PPV consistently describes both the space-charge-limited regime and the contact-limited regime as well as the transition between them. Recently, an alternative model, which includes an image force potential and small polaron hopping, has been proposed [38] as an explanation of our data shown in Figure 7.

It should be noted that the occurrence of an exponential distribution of interface states has also been observed in Schottky diodes made of inorganic semiconductors. The current-voltage characteristics of Au/GaAs, Cr/Si, Ni/Si, and Au/Si [39-41] exhibited a so-called T_0 anomaly: explanation of the experimental data required the addition of a constant temperature T_0 to the absolute temperature in the significant exponential part of the characteristic. From model calculations by Levine [42,43], it appeared that this T_0 anomaly defined by exponential surface-state energy distribution with a width that was related to the value of T_0. The broadened exponential tail of states at the interface indicates that these states are of extrinsic origin and as a result might be sensitive to the deposition conditions. In a recent study by Ioannidis et al. [44], it was demonstrated that the injection efficiency of Au contacts into a molecular doped polymer evolved from blocking to Ohmic over time. This evolution of charge injection has been attributed [44] to two main processes with time constants of a few hours and 1 month, respectively. The short process is consistent with an electronic reconfiguration of the molecules at the surface, which enhances interfacial charge transfer between the metal and the molecular material. The slow process might then arise from a polymer surface repair process. The observed evolution of injection and enhanced interfacial charge transfer might correspond to the formation and filling of interface states, as observed in our measurements. The question of how this exponential distribution of interface states depends on the processing conditions of the metal-polymer interface will be the subject of a further study.

V. SUMMARY

In conclusion, we have demonstrated that strongly contact-limited hole currents in PPV show Ohmic *J-V* characteristics. The hole density resulting from these *J-V* characteristics indicates that an exponential tail of localized states is formed at the polymer-electrode interface. The hole density at the electrode-polymer interface is then determined by the work function of the

electrode and the density of localized states at the interface. The question of whether such a tail of localized interface states is a general feature for evaporated metal contacts on conducting polymers will require more experimental data with a variation of both fabrication conditions and materials.

ACKNOWLEDGMENT

The authors thank M. J. M. de Jong and D. M. de Leeuw for offering valuable comments, as well as H. F. M. Schoo and R. C. J. E. Demandt for supplying the PPV. One author (M. C. J. M. V.) acknowledges the Dutch Science Foundation NWO/FOM for financial support.

REFERENCES

1. AR Brown, DDC Bradley, JH Burroughes, RH Friend, NC Greenham, PL Burn, AB Holmes, A Kraft, Appl Phys Lett 61:2793, 1992.
2. WR Salaneck, JL Brédas, Adv Mater 8:48, 1996.
3. IH Campbell, TW Hagler, DL Smith, JP Ferraris, Phys Rev Lett 76:1900, 1996.
4. RN Marks, DDC Bradley, Synth Met 57:4128, 1993.
5. ID Parker, J Appl Phys 75:1656, 1994.
6. PWM Blom, MJM de Jong, JJM Vleggaar, Appl Phys Lett 68:3308, 1996.
7. EH Rhoderick, RH Williams, Metal-Semiconductor Contacts. Oxford, UK: Clarendon Press, 1988.
8. PR Emtage, JJ O'Dwyer, Phys Rev Lett 16:356, 1966.
9. MA Lampert, P Mark, Current Injection in Solids. New York: Academic Press, 1970.
10. HK Henisch, Metal Rectifiers. New York: Oxford University Press, 1949, p. 98.
11. JG Simmons, Phys Rev Lett 15:967, 1965.
12. GG Malliaras, JC Scott, J Appl Phys 85:7426, 1999.
13. IH Campbell, PS Davids, DL Smith, NN Barashkov, JP Ferraris, Appl Phys Lett 72:1863, 1998.
14. EM Conwell, MW Wu, Appl Phys Lett 70:1867, 1997.
15. H Bässler, Polym Adv Technol 9:402, 1998.
16. MA Abkowitz, HA Mizes, JS Facci, Appl Phys Lett 66:1288, 1994.
17. YuN Gartstein, EM Conwell, Chem Phys Lett 255:93, 1996.
18. VI Arkhipov, EV Emelianova, YH Tak, H Bässler, J Appl Phys 84:848, 1998.
19. IH Campbell, TW Hagler, DL Smith, Phys Rev Lett 76:1900, 1996.
20. AJM Berntsen, Y Croonen, R Cuijpers, B Habets, CTHF Liedenbaum, HFM Schoo, RJ Visser, JJM Vleggaar, P van de Weijer, Proc SPIE 3148:264, 1997.
21. CC Wu, CI Wu, JC Sturm, A Kahn, Appl Phys Lett 70:1348, 1997.
22. M Löglund, P Dannetun, S Stafström, WR Salaneck, R Lazzaroni, C Frederiksson, JL Brédas, Phys Rev Lett 70:970, 1993.

23. M Löglund, JL Brédas, J Chem Phys 101:4357, 1994.
24. E Ettedgui, H Razafritimo, Y Gao, BR Hsieh, WA Feld, MW Ruckman, Phys Rev Lett 76:299, 1996.
25. Y Hirose, A Kahn, V Aristov, P Soukiassian, V Bulovic, SR Forrest, Phys Rev B 54:13748, 1996.
26. PWM Blom, MJM de Jong, MG van Munster, Phys Rev B 55:R656, 1997.
27. WD Gill, J Appl Phys 43:5033, 1972.
28. LB Schein, A Peled, D Glatz, J Appl Phys 66:686, 1989.
29. PM Borsenberger, J Appl Phys 68:6263, 1990.
30. MA Abkowitz, Phil Mag B 65:817, 1992.
31. H Bässler, Phys Status Solidi B 175:15, 1993.
32. L Pautmeier, R Richert, H Bässler, Synth Met 37:271, 1990.
33. YuN Gartstein, EM Conwell, Chem Phys Lett 245:351, 1995.
34. DH Dunlap, PE Parris, VM Kenkre, Phys Rev Lett 77:542, 1996.
35. SV Novikov, DH Dunlap, VM Kenkre, PE Parris, AV Vannikov, Phys Rev Lett 81:4472, 1998.
36. PWM Blom, MCJM Vissenberg, Mater Sci Eng (accepted).
37. JG Simmons, J Phys Chem Solids 32:1987, 1971.
38. MN Bussac, D Michoud, L Zuppiroli, Phys Rev Lett 81:1678, 1998.
39. FA Padovani, GG Summer, J Appl Phys 36:3744, 1965.
40. FA Padovani, J Appl Phys 37:921, 1966.
41. FA Padovani, J Appl Phys 38:891, 1967.
42. JD Levine, J Appl Phys 42:3991, 1971.
43. JD Levine, Solid-State Electronics 17:1083, 1974.
44. A Ioannidis, JS Facci, MA Abkowitz, J Appl Phys 84:1439, 1998.